



## THEORY ON THE FRINGE PATTERNS IN THE STUDY OF FERROELECTRIC DOMAIN WALLS USING ELECTRON HOLOGRAPHY

Wenwu Cao and Clive Randall  
Materials Research Laboratory, The Pennsylvania State University  
University Park, Pennsylvania 16802

Received March 10, 1993 by A. Pinczuk

The realization of electron holography provides a new powerful tool to probe the subtle and local changes of electric and magnetic fields inside a crystal structure through the phase variation of electron wave function. For a ferroelectric system the interference fringe patterns across a domain wall are very strongly affected by the presence of surface charge compensations. If the compensation is incomplete, a residue depolarization field will be present in the direction parallel to the electron beam, which can induce kink-like fringe bending. Earlier reported holographic images of ferroelectric domain walls revealed an asymmetry fringe bending. This behavior is explained through phase shifts induced by both the depolarization field and the strain field.

### 1 - Introduction

Electron holography provides us with a new methodology for the study of electric and magnetic field variations at the atomic scale.<sup>1</sup> In the past few years, the electron holography technique has demonstrated its power in the study of magnetic domain walls, p-n junctions, and fluxons in superconducting materials.<sup>2-7</sup> Recently, this method has been introduced into the study of ferroelectric materials, with particular interest to ferroelectric domain walls and defect dopants.<sup>8</sup> The kink-like phase change profile observed in the interference fringes qualitatively agree with the continuum theoretical descriptions of ferroelectric domain wall profiles.<sup>9,10</sup> However, quantitative agreement has not been obtained and the experimental results are not consistently reproducible. In this paper, a theoretical analysis is carried out, which intends to provide some basics for future studies on ferroelectric domain walls using electron holography.

Due to the existence of free charges, the study of polarization related electric field variations is much more complicated than the study of magnetic field variation using electron holography. The density of these free charges varies with the electric potential distribution and depends strongly on boundary conditions. The observed electron interference fringe patterns reflect the total electric potential distribution, therefore, in order to correlate them to the variation of polarization across a domain boundary one must separate different charge sources.

### 2 - Electron holography

The fundamental principle in electron holography is the interference of coherent high energy electrons. To a good approximation the

transmission of high energy electrons through a thin foil sample can be treated as a one-dimensional problem. Define  $z$  to be the electron traveling direction, then the phase change in the electron wave function due to the existence of an electric potential  $V(x_0, y_0, z)$  is given by

$$\phi(x_0, y_0) = \frac{2\pi}{\lambda} \int \left( \sqrt{1 - \frac{V(x_0, y_0, z)}{\Sigma}} - 1 \right) dz \quad (1)$$

where  $\lambda$  is the electron wave length,  $x_0$  and  $y_0$  define the point on the sample foil,  $\Sigma$  is the electron energy and  $V(x_0, y_0, z)$  represents the electric potential produced by the object. When the electron energy,  $\Sigma$ , is much greater than the magnitude  $|V(x_0, y_0, z)|_{\max}$  of the potential barrier, the phase shift of the electron wave can be simplified as<sup>11,12</sup>

$$\phi(x_0, y_0) = \frac{\pi}{\lambda \Sigma} \int V(x_0, y_0, z) dz \quad (2)$$

Since the energy of the electron beam is very large,  $\sim 200$  keV, Eq. (2) is usually sufficient to calculate the phase change.

The most important characteristic of a ferroelectric is a reversible spontaneous polarization. Generally, the spontaneous polarization results from a displacive or order-disorder phase transition. Without external electric fields, the macroscopic spontaneous polarization is developed in domains within the crystal, forming the so-called twin structures. There are two main types of twins. One has an inversion symmetry about the twin boundary but with equal strain in both variants. The second type is a twin of two variants with both different orientation of polarization and of spontaneous strain. The internal potential  $V(x_0, y_0, z)$  in a domain depends on the polarization and the boundary conditions at the crystal surfaces.

## 3 - Theory

From electrodynamics we know that the macroscopic electric field  $E$ , polarization  $P$ , and the electric displacement  $D$ , are all interrelated by the following equation,

$$D = \epsilon_0 E + P \quad (3)$$

Generally speaking, polarization  $P$  depends on local electric field which is different from the macroscopic electric field  $E$ . A ferroelectric system has a number of additional considerations owing to the spontaneous polarization and boundary conditions. Two extreme cases are shown below to illustrate this situation. For simplicity we assume the spontaneous polarization,  $P_0$ , is perpendicular to the sample plane.

Case I. Complete charge compensation

The simplest case is when the sample surfaces are electroded and the two electrodes were short circuited during the development of the spontaneous polarization. For this system we have the condition  $E = 0$ , so that

$$D_0 = P_0 \quad (4)$$

Since  $P_0 \cdot n$  is the surface "bound charge" density and  $-D_0 \cdot n$  equals the surface "free charge" density, the polarization is completely compensated by the generated free charges. The system is in equilibrium and has a fully developed spontaneous polarization throughout the whole crystal. When the temperature is kept constant, there is no macroscopic electric field present either inside or outside of the ferroelectric crystal. Therefore, no fringe variations are expected.

Case II. Completely uncompensated polarization

The other simple but unrealistic case is the polarization being completely uncompensated, i.e.,  $D = 0$ . Then there will be a very strong depolarization field being produced inside the sample,

$$E = -P_0 / \epsilon_0 \quad (5)$$

which is equal to the microscopic field. This field is too large to be sustained. For example, the polarization of  $BaTiO_3$  is  $18 \mu C/m^2$ , from Eq.(5) the depolarization field can be as large as  $2 \times 10^8$  V/cm. Under such a large field, either the polarization will be destroyed (which suppress the structural phase transition) or the system will obtain free charges (from the environment or within the crystal) to reduce the field level.

As free charges are readily available, a real system is more like Case I above, even when the sample is not being electroded. This is to say that the phase shift induced by the depolarization field difference across a domain boundary is being counterbalanced by the phase shift produced by the field of compensation charge. However,

charge compensation in a non-electroded sample is a relaxation process, the rate can be very slow as the equilibrium is approached. In addition, since most of the ferroelectrics are also improper ferroelastic, a small level of the depolarization field could be sustained through elastic distortion of the structure. In other words, the system is sometimes not fully compensated, at least in a finite time period. This situation can also happen in an already compensated system through the change of temperature (pyroelectric effect) or mechanical stress (piezoelectric effect).

The depolarization field in the partially compensated system can be expressed as

$$E = -(P_0 - D) / \epsilon_0 = -(1 - \eta) P_0 / \epsilon_0 \quad (6)$$

Here we have defined a compensation factor  $\eta = D/P_0$  (in our problem the vectors  $D$  and  $P_0$  are in the same direction) which is less or equal to unity,  $0 < \eta \leq 1$ . The compensation factor  $\eta$  depends strongly on temperature, stress, and also on time. Since the net field in Eq. (6) is non-zero if  $\eta < 1$ , and proportional to the polarization, one may use holographic electron microscopy to study the variation of polarization inside a twin domain structure, through the residue field and the associated phase shift. The basic requirement is that  $\eta$  changes slowly with time.

The associated spontaneous polarization profiles can be determined using Landau-Ginsburg theory. As an example, in a  $180^\circ$  twin structure with the polarization in the  $z$ -direction (the electron beam direction), the profile can be described by<sup>10</sup>

$$P(x) = \frac{P_0 \sinh(x/\xi)}{\sqrt{A + \sinh^2(x/\xi)}} \quad (7)$$

where  $x$  is the space variable in the domain wall normal direction and  $\xi$  is the characteristic width of the domain wall; the parameter  $A$  is a constant which reflects the sharpness of the first order transition. For a second order phase transition  $A = 1$  and Eq. (9) reduces to a hyperbolic tangent function<sup>9</sup>

$$P = P_0 \tanh(x/\xi) \quad (8)$$

From Eqs. (2), (6), and (7) or (8), one can calculate the phase profile across a domain wall:

$$\Delta\phi(x_0) = \frac{(1-\eta)\pi}{\lambda\Sigma} P_z^2(x_0) \quad (9)$$

Here  $x_0$  defines the coordinate on the sample surface and the phase reference is chosen at the domain wall center. Since phase variations are proportional to the polarization, the fringe patterns should be kink-like as observed in  $BaTiO_3$ .<sup>8</sup> For later convenience, we define these kink-like patterns as type I fringes for domain walls, which is antisymmetric.

Most ferroelectrics are also improper

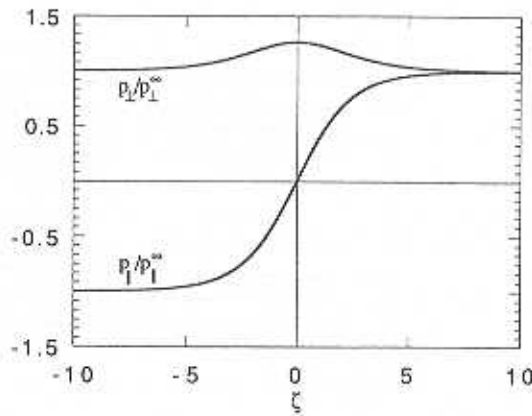


Fig. 1. The polarization profiles for the polarization components perpendicular and parallel to the domain wall in a  $90^\circ$  twin structure.

ferroelastics, i.e., the strain is the secondary order parameter and coupled to the polarizations; hence, it also changes in the domain wall region. The relationship between the spontaneous polarization  $\mathbf{P}$  and the spontaneous strain  $\tilde{\mathbf{S}}$  can be written as:

$$S_{ij} = Q_{ijkl} P_k P_l \quad (i, j, k, l = 1, 2, 3) \quad (10)$$

where  $Q_{ijkl}$  is the electrostriction constant. The non-zero strain components are defined by the crystal symmetry and boundary conditions. For the  $180^\circ$  ferroelectric twin discussed above the strain variation in the domain wall region is<sup>10,13</sup>

$$\Delta S_{ij} = Q_{ij33} (P_\infty^2 - P^2(x)) \quad (11)$$

Due to the symmetric nature of Eq.(11), the phase profile reflecting the strain variation will be symmetric about the center of the domain wall. We define the hump-like symmetric fringes as type II fringes for domain walls. Additional contribution to the type II fringes may come from the polarization component perpendicular to the domain wall, which is non-zero for all non- $180^\circ$

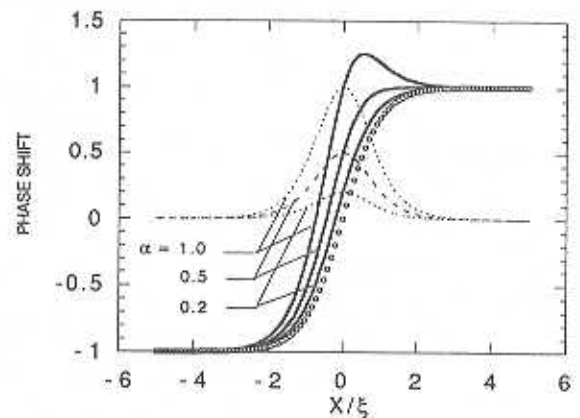


Fig. 2. Variation of the total phase shift profile with respect to the ratio  $\alpha = |\Delta\phi_0|/|\Delta\phi_\infty|$  of contributions from Type I and Type II.

domain walls. The profile of this component is hump-like as illustrated in Fig. 1. Also, because the strong polarization gradient at the domain wall region, charge defects and vacancies tend to be trapped by the domain walls, these point charge defects can also contribute to the type II fringes as summarized in Table I.

In general, the fringe patterns observed across a ferroelectric domain wall will be a mixture of type I and type II, so that the resultant fringe patterns will be non-symmetric. For example, assuming the polarization is given by Eq. (8), then the resultant normalized fringe profile is illustrated in Fig. 2. The circles in Fig. 2 represent type I profile and the dashed lines represent type II profile,  $\alpha = |\Delta\phi_0|/|\Delta\phi_\infty|$  is the ratio of the maximum phase shifts of type II versus type I. One can see that the resultant phase shift becomes more and more asymmetric as  $\alpha$  increases from 0 to 1, and the total profile moves to the left. This asymmetric feature is obviously seen in the results reported in ref. 8 for  $\text{BaTiO}_3$  (see the data points in Fig. 3). According to the above analysis, we propose the fringes to be fitted in the following equation:

Table I

	Shape	Symmetry	Source of Contribution
Type I		Antisymmetric	Polarization parallel to domain wall
Type II		Symmetric	Polarization perpendicular to domain wall; point charge defects; strain variation across the domain wall

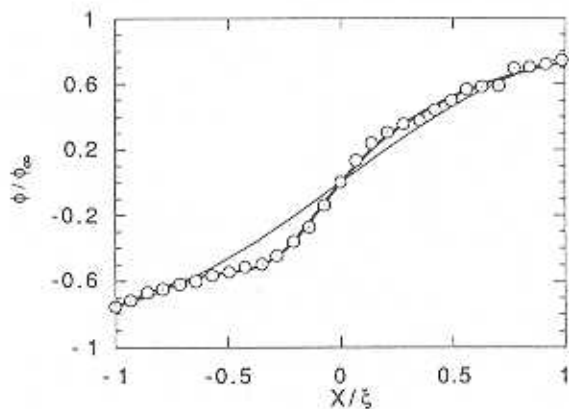


Fig. 3. Comparison of the theory with the experimental data of ref. 8. The circles are the experimental data, the thin line is the fitting to a simple hyperbolic tangent and the thick line was obtained using Eq. (12).

$$\Delta\phi(x)/\Delta\phi_{\infty} = \tanh\left(\frac{x-x_d}{\xi}\right) + \alpha \left(1 - \tanh^2\left(\frac{x-x_d}{\xi_s}\right)\right) + \beta \quad (12)$$

where  $x_d$  and  $\beta$  are respectively the horizontal and vertical deviations of the domain wall center from the reference center used in the experiment. A different characteristic length  $\xi_s$  for the type II fringe is introduced, which may not be the same as  $\xi$ . Fig. 3 shows the comparison between the fitting of ref. 8 (thin line) and the fitting using Eq. (12) [thick line]. One can see that the current fitting is quite satisfactory with the following fitting parameters:  $x_d = -0.285 \xi$ ;  $\alpha = -0.323$ ;  $\xi_s = 0.31 \xi$  and  $\beta = -0.1285$ . Here we like to emphasize that the functional form for the first order phase transition in  $\text{BaTiO}_3$  would be more appropriate to use eq. (7) instead of eq. (8) if the constant A can be determined.

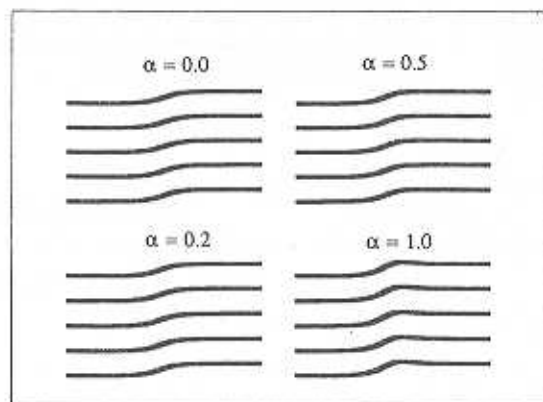


Fig. 4. Calculated fringes across a domain wall for different  $\alpha$  assuming  $|\Delta\phi_0| = \pi/2$ .

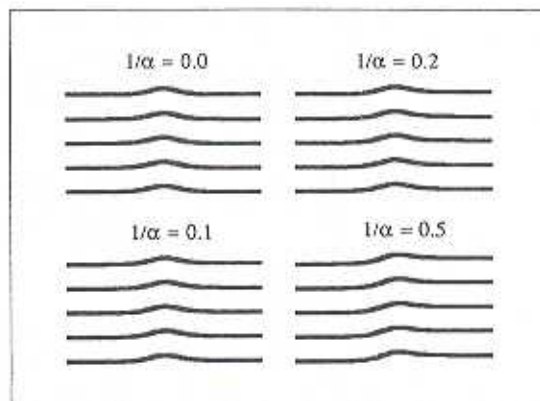


Fig. 5. Calculated fringes across a domain wall for different  $\alpha$  assuming  $|\Delta\phi_0| = \pi/2$ .

Figures 4 and 5 show some of the expected fringe patterns across a ferroelectric domain wall using the current analysis. The fringes in Fig. 4 were calculated by assuming  $|\Delta\phi_{\infty}| = \pi/2$  while the fringes in Fig. 5 were calculated by assuming  $|\Delta\phi_0| = \pi/2$ . One can see the nature of the fringes changes from type I to type II as the parameter  $\alpha$  increases from 0 to  $\infty$ .

#### 4 - Conclusions

As the electron holography technique is very sensitive to the local electric potential variations, the incompletely compensated depolarization field in domain wall regions can be measured. The fringe patterns can be directly correlated to the space profile of polarization variation in a twin structure. The sample should not be electroded and the electron energy must be very high. For a compensated sample, one may vary the temperature to destroy the charge balance and make the domain wall visible through the electron phase shift. In general, the fringe bending observed is a mixture of type I and type II, one must separate the two types of contributions in order to extract useful information from electron holography. Eqs. (9) and (12) can be used to fit the fringe patterns across a  $180^\circ$  and a non- $180^\circ$  domain wall, respectively.

#### Acknowledgments

The author is indebted to Drs. X. Zhang, D. Joy and L. F. Allard for many helpful discussions on the electron holography technique and Dr. L. E. Cross for discussions on ferroelectrics. This research was supported by Air Force Office of Scientific Research under Grant No. AFOSR-91-0433.

## References

1. A. Tonomura, *Rev. Mod. Phys.*, **59**, 639 (1987).
2. S. Frabboni, G. Matteucci, and G. Pozzi, *Phys. Rev. Lett.*, **55**, 2196 (1985).
3. A. Tonomura, T. Matsuda, J. Endo, J. Ariei, and K. Mihama, *Phys. Rev. Lett.*, **44**, 1430 (1980).
4. A. Fukuhara, K. Shinagawa, A. Tonomura, and H. Fujiwara, *Phys. Rev. B*, **27**, 1839 (1983).
5. A. Tonomura, T. Matsuda, R. Suzuki, A. Fukuhara, N. Osakabe, H. Umezaki, J. Endo, K. Shinagawa, Y. Sugita, and H. Fujiwara, *Phys. Rev. Lett.*, **48**, 1443 (1982).
6. A. Tonomura, N. Osakabe, T. Matsuda, K. Kawasaki, R. Suzuki, J. Endo, S. Yano and H. Yamada, *Phys. Rev. Lett.*, **56**, 792 (1986).
7. M. Tsuyoshi, A. Tonomura, R. Suzuki, J. Endo, N. Osakabe, H. Umezaki, H. Tanabe, Y. Sugita and H. Fujiwara, *J. Appl. Phys.*, **53**, 5444 (1982).
8. X. Zhang, T. Hashimoto and D. C. Joy, *Appl. Phys. Lett.*, **60**, 784 (1992).
9. V. A. Zhirnov, *Sov. Phys. JETP*, **35**, 822 (1959).
10. W. Cao and L. E. Cross, *Phys. Rev. B*, **44**, 5, (1991).
11. G. F. Missiroli, G. Pozzi, and U. Valdrè, *J. Phys. E*, **14**, 549 (1981).
12. M. Yanzi, *Optik*, **68**, 319 (1984).
13. W. Cao and G. R. Barsch, *Phys. Rev. B*, **41**, 4334 (1990).